Environmental Science & Technology

pubs.acs.org/est

Article

COVID-19-Induced Lockdowns Indicate the Short-Term Control Effect of Air Pollutant Emission in 174 Cities in China

Dawei Lu, Jingwei Zhang, Chaoyang Xue, Peijie Zuo, Zigu Chen, Luyao Zhang, Weibo Ling, Qian Liu,* and Guibin Jiang

Cite This: *Environ. Sci. Technol.* 2021, 55, 4094–4102

Read Online

ACCESS | Metrics & More | Article Recommendations | Supporting Information

ABSTRACT: The contradiction between the regional imbalance and an one-size-fits-all policy is one of the biggest challenges in current air pollution control in China. With the recent implementation of first-level public health emergency response (FLPHER) in response to the COVID-19 pandemic in China (a total of 77 041 confirmed cases by February 22, 2020), human activities were extremely decreased nationwide and almost all economic activities were suspended. Here, we show that this scenario represents an unprecedented "base period" to probe the short-term emission control effect of air pollution at a city level. We quantify the FLPHER-induced changes of NO_2, SO_2, $PM_{2.5}$, and PM_{10} levels in 174 cities in China. A machine learning prediction model for air pollution is established by coupling a generalized additive model, random effects meta-analysis, and weather research and forecasting model with chemistry analysis. The short-term control effect under the current energy structure in each city is estimated by comparing the predicted and observed results during the FLPHER period. We found that the short-term emission control effect ranges within 53.0%−98.3% for all cities, and southern cities show a significantly stronger effect than northern cities ($P < 0.01$). Compared with megacities, small−medium cities show a similar control effect on NO_2 and SO_2 but a larger effect on $PM_{2.5}$ and PM_{10}.

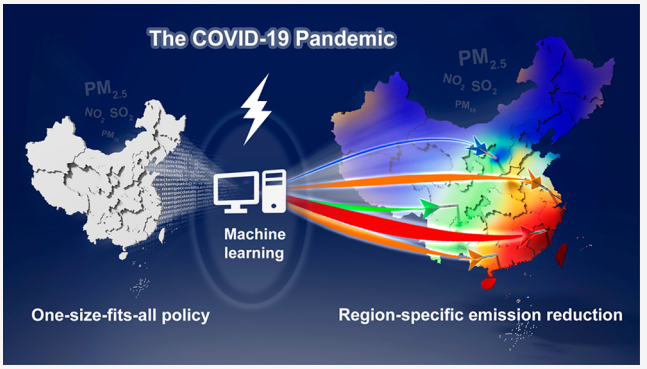

KEYWORDS: *COVID-19, air pollution, machine learning, emission reduction, public health emergency*

1. INTRODUCTION

Air pollution is a notable environmental health risk in China that has been estimated to cause ~1.1 million premature deaths annually.[1,2] To improve air quality and protect human health, the China government has developed a series of strict air pollution control actions since 2013 with the goal to reduce the emissions of air pollutants (i.e., ambient particulate matter with an aerodynamic diameter <2.5 μm ($PM_{2.5}$) and <10 μm (PM_{10}), sulfur dioxide (SO_2), and nitrogen oxides (NO_x)) across the country.[3−7] After strong policy regulation, the average $PM_{2.5}$ concentration in China has been dramatically reduced from 89.5 $\mu g/m^3$ in 2013 to 43 $\mu g/m^3$ in 2019. However, this still much exceeded the WHO guideline limit (10 $\mu g/m^3$) and the grade I level of the Chinese Ambient Air Quality Standards (35 $\mu g/m^3$).

In the current air pollution control in China, one of the biggest challenges is the contradiction between the regional imbalance and the one-size-fits-all policy. The energy structure and economy levels vary greatly in different regions in China, leading to largely varied emission and pollution levels. Thus, the one-size-fits-all policy inevitably results in a low efficiency of pollution control or waste of resources. Until now, it has been still difficult to predict the effectiveness of regional air pollution control policies. For future clean air actions, it is crucial to estimate the city-specific effectiveness of emission control measures and adjust policies to local conditions.

The recent outbreak of the corona virus disease 2019 (COVID-19) provided an unexpected scenario for this purpose. The COVID-19 was first reported in Hubei Province in China in December 2019,[8] and then, the number of confirmed cases increased in other provinces in January 2020. In January 23, 2020, the first-level public health emergency response (FLPHER) was triggered to cut down the rapid spread of COVID-19 throughout China.[9] During the period of FLPHER, stringent restriction measures on the mobility of the citizens were implemented.[10] Except for some mainstay sectors

Special Issue: Environmental Transmission and Control of COVID-19

Received: October 23, 2020
Revised: March 16, 2021
Accepted: March 18, 2021
Published: March 26, 2021

that maintained the basic human living and society operating, traffic, construction, commercial, and industrial activities were subjected to an extreme or complete standstill.[11] As a response, the emission of air pollutants from anthropogenic sources[12−14] showed a substantial reduction.[15−27] The similar phenomenon was also observed in other countries during the global spread of the COVID-19 pandemic.[27,28] Noteworthily, the strict FLPHER measures were implemented nationwide rather than regionally. Therefore, we hypothesize that the COVID-19 pandemic can be used as an unprecedented "base period" to estimate the short-term control effect of different cities for developing city-specific emission control measures.

Here, we use a machine learning prediction model to simulate the air pollution levels (NO_2, SO_2, $PM_{2.5}$, and PM_{10}) in 174 cities in China (involving a population of ∼1 billion; see Figure S1) on the basis of meteorological factors, atmospheric environmental chemistry process, and emission inventory data. Assuming the FLPHER period (January 23−February 22, 2020) with COVID-19 lockdowns as a base period, we quantify the city-level and species-specific short-term control effect by the difference between the predicted and observed results. Here, the short-term control effect is defined as the reduction degree of air pollution by short-term administrative means for a specific city under the current energy structure. In fact, the short-term administrative means have been proven to take effect in some past special events, such as the "Olympic Blue" during the 2008 Beijing Summer Olympic Games and the "APEC Blue" during the 2014 Beijing Asia-Pacific Economic Cooperation (APEC) Economic Leaders' Meetings.[29−31] It is worth noting that the COVID-19 lockdowns mainly reduced the emissions from traffic and industrial sectors but less affected the power and residential sectors, because the two latter are the basic sectors to maintain the society operating. Therefore, the short-term control effect may not reflect the maximum potential of pollution reduction for a city. However, as an estimate of the effectiveness of short-term stringent emission control, it provides an important quantitative reference for devising target policies of city-specific air pollution regulation. Especially, considering that the COVID-19 severity may affect the emission reduction in a city, we paid particular attention to the difference between the Hubei province and out of the Hubei province due to the much more severe COVID-19 situation in Hubei.

2. METHODS

Study Regions and Sources of Data. We investigated 174 cities in 26 provinces, encompassing 99% of the COVID-19 cases (by February 22, 2020) in mainland China. The number of daily confirmed COVID-19 cases in 174 cities in China were obtained from the National Health Commission of the PR China. The observation data of air pollutants (i.e., NO_2, SO_2, $PM_{2.5}$, and PM_{10}) in these cities were collected from the Chinese National Environmental Monitoring Center (CNEMC). The ambient temperature (AT) and relative humidity (RH) data were obtained from the National Meteorological Centre of the PR China.

Generalized Additive Model and Random Effects Meta-Analysis. We used the generalized additive model, which enables the evaluation of the associations between the concentrations of air pollutants and the daily number of confirmed COVID-19 cases. This model was conducted by R software (version 3.6.2). The detailed framework of this model can be described as follows:

$$\log E(O_t) = \beta C_t + \mathrm{ns}(\mathrm{AT}, \mathrm{df}) + \mathrm{ns}(\mathrm{RH}, \mathrm{df}) + \alpha \quad (1)$$

$$\mathrm{RR} = \exp(\beta) \quad (2)$$

where O_t and C_t represent the daily mean concentration of an air pollutant and daily confirmed COVID-19 cases on day t, respectively; $E(O_t)$ represents the expected value of the concentration of air pollutant on day t; β is the regression coefficient; α is the intercept; AT and RH represent the ambient temperature and relative humidity on day t, respectively; ns represents the natural smooth functions of the model. Herein, we used 3 day moving averages of AT and RH as 3 degrees of freedom (df) to control the potential effects of ambient temperature and humidity. The relative response factors (RR) with 95% confidence intervals (CIs) were used to describe the changes of the levels of air pollutants with per 10 confirmed COVID-19 cases increasing. RR > 1 indicates a positive response, and RR < 1 indicates negative response. The exp represents an exponential function. Considering that the lifetimes of the air pollutants in the atmosphere are normally in the range of several days to 1 week, we used a period of 7 days to estimate the lag effects (from lag day 1 to lag day 7) of air pollution in response to COVID-19 cases. Then, subgroup analysis for different cities was performed with random effects meta-analysis through R software (version 3.6.2).

WRF-Chem Model Analysis. The weather research and forecasting model coupled with chemistry analysis (WRF-Chem) (version 3.7.1) was used to predict the concentrations of air pollutants under the real meteorological conditions but assuming no COVID-19-caused lockdowns in China.[32−34] The domains, physical, and chemical schemes are given in Figure S1 and Table S1. The meteorological initial and boundary conditions (every 6 h) were obtained from the National Centers for Environmental Prediction (NCEP) 1° × 1° Final Reanalysis Data (FNL).[35] The initial and chemical boundary conditions (every 6 h) were obtained by the Global Simulations of Whole Atmosphere Community Climate Model (WACCM).[36] The mosaic Asian anthropogenic emission inventory (2010) and Multi-Resolution Emission Inventory for China (2016) were used in the WRF-Chem modeling.[37,38] The NH_3 and biomass burning emission data were adopted from previous studies,[39,40] and biogenic emission was calculated using the Model of Emissions of Gases and Aerosols from Nature (MEGAN).[41] The data set of emissions were the last version available.

We used the data of the investigated cities from the databases mentioned above over the period of November 14, 2019−January 22, 2020 to train the model by altering the emission rates (to 80% for SO_2, 50% for NH_3, and 50% for the direct emissions of $PM_{2.5}$ and PM_{10}) throughout the domain, until the predicted results well-matched the observed results (Figure 3 and Figure S2). The mean bias (MB), root-mean-square error (RMSE), and the index of agreement (IOA) were used to assess the predictions against observations:

$$\mathrm{MB} = \frac{1}{N}\sum_{i=1}^{N}(P_i - O_i) \quad (3)$$

$$\mathrm{RMSE} = \left[\frac{1}{N}\sum_{i=1}^{N}(P_i - O_i)^2\right]^{1/2} \quad (4)$$

https://doi.org/10.1021/acs.est.0c07170
Environ. Sci. Technol. 2021, 55, 4094−4102

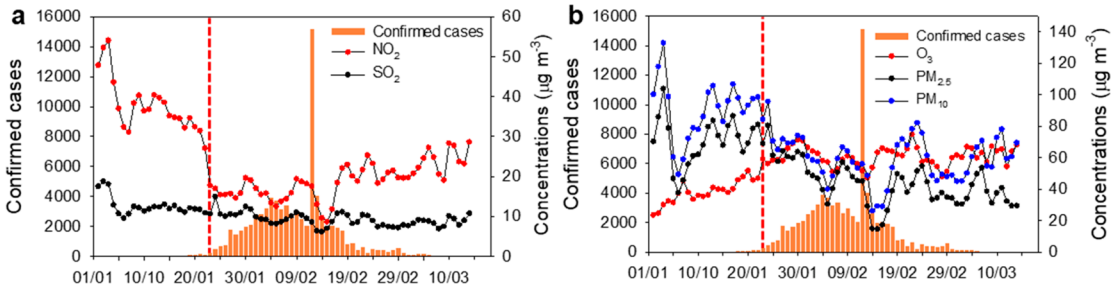

Figure 1. Time evolution of daily pollution levels of NO_2, SO_2, O_3, $PM_{2.5}$, and PM_{10} and daily confirmed COVID-19 cases in 174 cities in China during the first-level public health emergency response (FLPHER) lockdown period. (a) Daily mean NO_2 and SO_2 concentrations. The error bars represent standard deviations (1SD) of 24 measurements in a day (n = 24). (b) Daily mean $PM_{2.5}$, PM_{10}, and O_3 concentrations. The error bars represent standard deviations (1SD) of 24 measurements in a day (n = 24). The red dashed lines in a and b represent the date of the first implementation of lockdowns due to the COVID-19 outbreak in Wuhan, China.

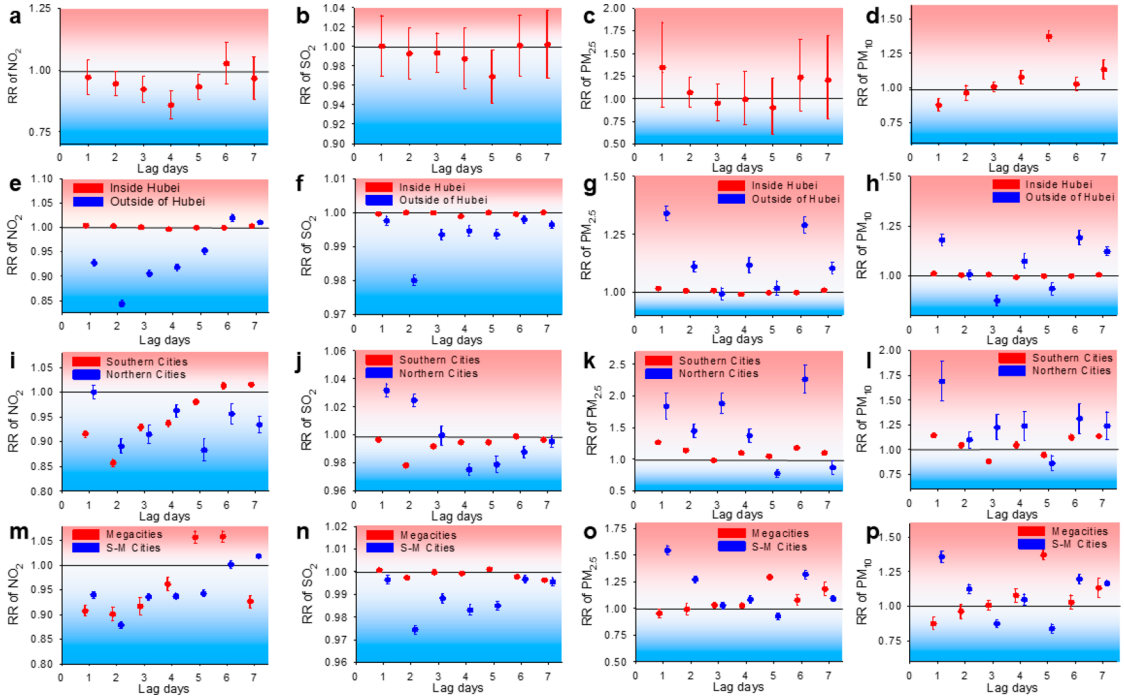

Figure 2. Associations between the levels of four air pollutants and confirmed COVID-19 cases in 84 cities (with more than 30 total confirmed cases) in China during the FLPHER period. (a−d) Overall all-city relative response factor (RR) values of (a) NO_2, (b) SO_2, (c) $PM_{2.5}$, and (d) PM_{10} to the confirmed COVID-19 cases. (e−p) Comparison of the RR values of NO_2, SO_2, $PM_{2.5}$, and PM_{10} to the confirmed COVID-19 cases (e−h) between the cities in and outside of the Hubei province, (i−l) southern and northern cities, and (m−p) megacities and small−medium (S−M) cities. Note that the results represent the RR values and the 95% confidence intervals (CIs) per 10 newly confirmed COVID-19 cases.

$$\mathrm{IOA} = 1 - \frac{\sum_{i=1}^{N}(P_i - O_i)^2}{\sum_{i=1}^{N}(|P_i - \bar{O}| + |O_i - \bar{O}|)^2} \quad (5)$$

where P_i and O_i represent the predicted and observed variables, respectively, N is the total number of the simulations for comparison, and $\bar{o}$ represents the average-observations.

Estimate of the Short-Term Emission Control Effect. The short-term control effect of air pollutants (ΔEP) for each city was estimated by the following equation:

$$\Delta \mathrm{EP}_t = \mathrm{ObsP}_t - \mathrm{SimP}_t \quad (6)$$

where $\Delta \mathrm{EP}_t$ represents the short-term emission control effect on air pollutants (e.g., NO_2, SO_2, $PM_{2.5}$, and PM_{10}) on day t; ObsP_t represents the monitored real concentration of the air pollutants on day t; and SimP_t represents the predicted concentration of the air pollutants by the WRF-Chem model under an assumed scenario without COVID-19 lockdowns.

3. RESULTS AND DISCUSSION

Air Quality Trends during the COVID-19 Pandemic Period in China. As shown in Figure 1, the daily average concentration of air pollutants in China showed a remarkable variation with the outbreak of COVID-19. The average levels of NO_2, $PM_{2.5}$, PM_{10}, SO_2, and ozone (O_3) in 174 cities were 37.8 ± 6.7, 70.6 ± 15.3, 90.7 ± 19.3, 12.6 ± 2.4, and 38.2 ± 7.3 $\mu g/m^3$ prior to the implementation of the FLPHER, which were close to the same-term mean pollution levels of 2019. Notably, after the FLPHER was triggered, dramatic variation trends were observed for these air pollutants. The average concentrations of NO_2, PM_{10}, $PM_{2.5}$, and SO_2 in these cities decreased considerably by 56.5% (16.4 ± 3.4 $\mu g/m^3$), 33.9% (59.9 ± 16.1 $\mu g/m^3$), 33.7% (46.9 ± 15.8 $\mu g/m^3$), and 22.9%

https://doi.org/10.1021/acs.est.0c07170
Environ. Sci. Technol. 2021, 55, 4094−4102

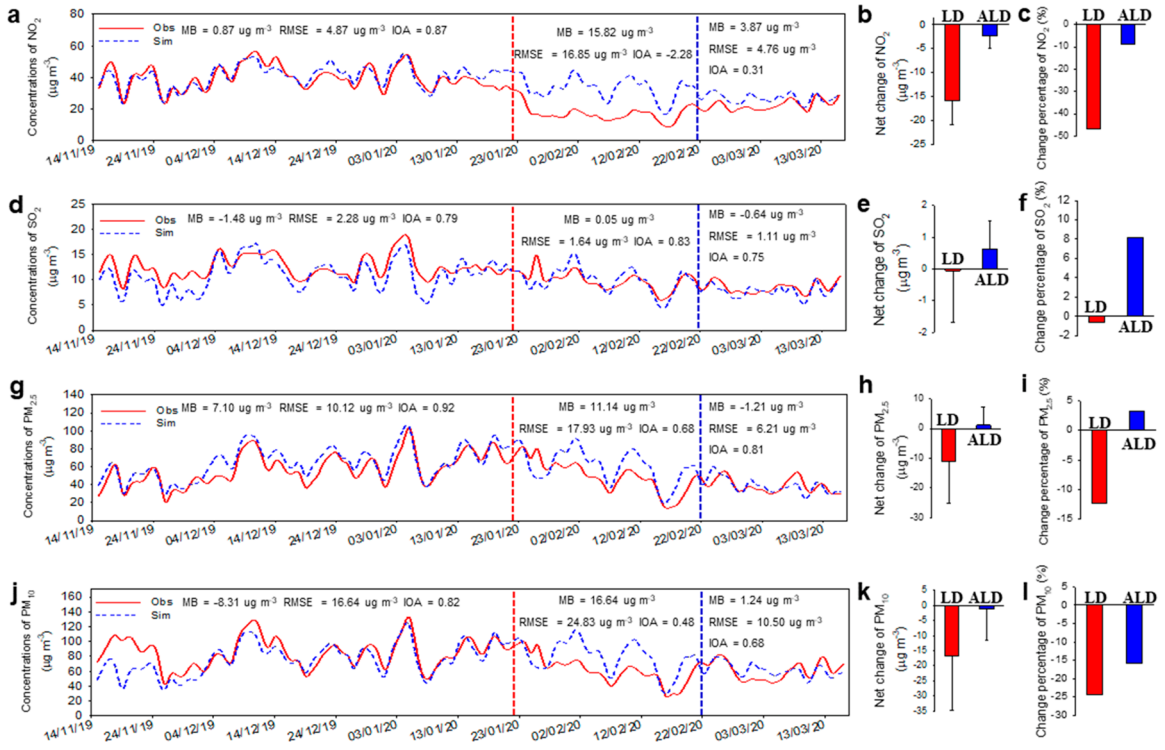

Figure 3. WRF-Chem model-simulated and observed average concentrations of major air pollutants in 174 cities in China. The simulation (dotted blue line) was performed with assuming no outbreak of COVID-19 lockdowns against the real observation (red solid line). (a, d, g, and j) Daily mean concentrations of (a) NO_2, (d) SO_2, (g) $PM_{2.5}$, and (j) PM_{10} for observation and simulation from November 14, 2019 to March 15, 2020. Period I (November 14, 2019−January 22, 2020) before the implementation of FLPHER lockdowns was used as a training set to optimize the model. Period II (January 23, 2020−February 20, 2020) and Period III (February 21, 2020−March 15, 2020) represent the FLPHER lockdown period (test set) and recovery period when most cities rescinded the FLPHER lockdowns (validation set). (b, e, h, and k) Difference between the observed and simulated average concentrations of (b) NO_2, (e) SO_2, (h) $PM_{2.5}$, and (k) PM_{10} in 174 cities during Periods I and II. The error bars represent standard deviations (1SD) during Period II (n = 28) and Period III (n = 24). (c, f, i, and l) Change percentage (%) between the observed and simulated average concentrations of (c) NO_2, (f) SO_2, (i) $PM_{2.5}$, and (l) PM_{10} in 174 cities during Periods II and III. The LD and ALD represent the FLPHER lockdown period (Period II) and after the FLPHER lockdown period (Period III), respectively.

(9.72 ± 1.77 $\mu g/m^3$), respectively, while, on the contrary, the O_3 concentration significantly increased by 59.6% (60.9 ± 6.3 $\mu g/m^3$). These results indicate that the city lockdowns (CLDs) indeed exerted a significant impact on pollutant emissions.

With regard to individual pollutants, ground-level O_3 is influenced by nonlinear chemical processes of NO_x and volatile organic compounds (VOCs) and NO-titration, rather than being directly emitted from certain sectors.[29,42,43] Thus, the change of O_3 was not used to assess the emission control effect in this study. It should be noted that the air pollutants have certain lifetimes (normally several days) in the atmosphere and humans normally have a response time to peak cases, so the responses of air pollution to COVID-19 lockdowns had a lagging effect. Consequently, the minimum concentrations of NO_2, SO_2, $PM_{2.5}$, and PM_{10} did not occur on the day but lagged behind the day when the daily confirmed COVID-19 cases reached the peak point in a city.

Direct Response of Air Pollution to Confirmed COVID-19 Cases. To verify the responses of air pollutants to the COVID-19 lockdowns, we further investigated the associations between the pollution levels and confirmed COVID-19 cases over 84 cities (with total confirmed cases >30) in China. Here, we define a relative response factor (RR) to describe the lagging effect between air pollutants and confirmed COVID-19 cases (see the Methods section, eqs 1 and 2 for details). The RR > 1 indicates a positive response, and RR < 1 indicates a negative response. Both the absolute values and changing trends of RR are concerned.

As shown in Figure 2a−c, the RR values of NO_2, SO_2, and $PM_{2.5}$ to the increase of confirmed COVID-19 cases showed a decline trend during the initial several days. This was consistent with the decreasing trends of levels of these air pollutants (NO_2, SO_2, and $PM_{2.5}$) during the FLPHER period (Figure 1). For the overall pooled estimate of 84 cities, the negative response of NO_2 to the increase of confirmed COVID-19 cases was the strongest among the concerned air pollutants, and the lowest RR value of 0.86 (95% confidence interval (CI): 0.80, 0.92) was obtained at lag day 4. Note that 4 days significantly exceed the lifetime of NOx in the atmosphere (~1 day), which could be attributed to the lagging time between peak cases and human responses. The lowest RR values for $PM_{2.5}$ and SO_2 were achieved at lag day 5 ($RR_{PM_{2.5}}$ = 0.86 and RR_{SO_2} = 0.97). Notably, $PM_{2.5}$ showed positive RR values at initial 2 days, probably because the sources of $PM_{2.5}$ pollution were more complex than those of NO_2 and SO_2 (including secondary formation from gaseous precursors), and thereby, its negative response to the COVID-19 lockdown was slower than those of NO_2 and SO_2. Despite that, the RR of $PM_{2.5}$ also showed a decline trend, indicating that the COVID-19 lockdown still greatly affected the $PM_{2.5}$ pollution. After the lag days when the RR of pollutants reached the lowest values, the impact of the COVID-19 lockdowns was

https://doi.org/10.1021/acs.est.0c07170
Environ. Sci. Technol. 2021, 55, 4094−4102

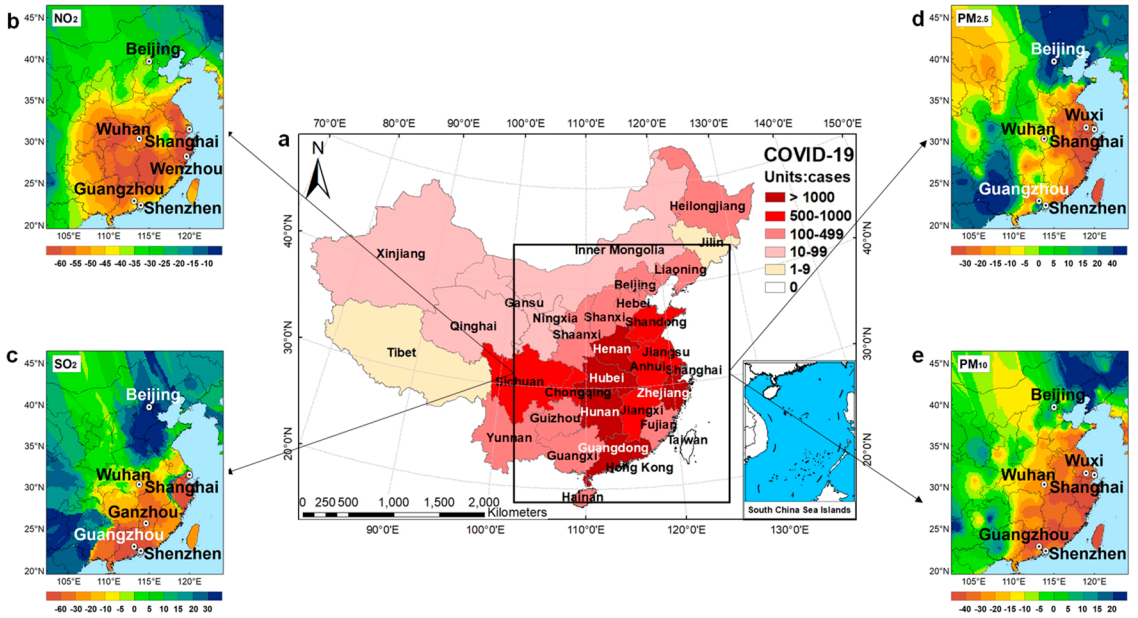

Figure 4. National scale short-term control effect of air pollutants derived from the COVID-19 lockdowns. (a) Cumulative confirmed COVID-19 cases in different provinces in China before February 22, 2020. (b–e) Estimated short-term control effects of (b) NO_2, (c) SO_2, (d) $PM_{2.5}$, and (e) PM_{10} in China. The different colors represent different short-term control effects, and a darker yellow (i.e., more negative value) represents a larger short-term emission reduction.

gradually weakened, so the RR values appeared to increase. Regarding PM_{10}, its RR value showed an increasing trend from 0.87 at lag day 1 to 1.37 at lag day 5 (Figure 2d), indicating that the main emitting sectors associated with PM_{10} were different from those of NO_2, SO_2, and $PM_{2.5}$. The positive responses suggested that these sectors were less restricted by the FLPHER regulations.

We then investigated the response of air pollutants to the COVID-19 cases in different cities, stratified by geographic location and city scale. Figure 2e–h shows weaker responses in cities of the Hubei province than those outside of the Hubei province. This difference can be explained by the facts that the RR values were calculated on the basis of per 10 confirmed COVID-19 cases increasing and that Hubei had a large number of cases. Furthermore, southern cities showed lower RR values for the air pollutants relative to northern cities (Figure 2i–l). It is interesting to note that $PM_{2.5}$ and PM_{10} had more significantly negative responses (i.e., lower RR values than 1) to the outbreak of COVID-19 in megacities (i.e., cities with a population exceeding 10 million[44]) than in small–medium cities (S–M cities), whereas SO_2 and NO_2 had lower RR values in small–medium cities than in megacities (Figure 2m–p). The results mentioned above indicate that the chemical species and sources of air pollution in China were distinctly different in different cities.

Estimate of Regional Short-Term Emission Control Effect. To quantify the short-term control effects of COVID-19 lockdowns on the pollutant emission, we conducted model simulations using weather research and forecasting model with chemistry (WRF-Chem model) analysis. Then, we predicted the temporal pollution trends in the case of no outbreak of COVID-19 or associated lockdowns. The simulations of air pollution levels were performed on the basis of meteorological factors, atmospheric environmental chemistry processes, and emission inventory data by the WRF-Chem model.[45−47]

We first trained the model by using the temporal evolution of air pollution from November 14, 2019 to January 22, 2020 as a training set. The meteorological factors (e.g., wind field; Figure S2) were coupled in this simulation. As shown in Figure 3a,d,g,j, the simulated data were highly consistent with the observed. Moreover, the temperature and relative humidity data modeled by the WRF-Chem model well-matched the monitored data (Figure S3), also suggesting that the modeling is reliable. Then, the levels of the air pollutants during the period after February 22, 2020 were used as a validation set for the WRF-Chem model (see Figure 3). After that date, in most cities, the FLPHER was rescinded and the transportation, construction, and industrial activities were gradually restarted. As shown in Figure 3, the simulated results were also close to the observed results for the validated set. All the above results verified the accuracy and robustness of the WRF-Chem model for the air pollution. Considering that the COVID-19-caused FLPHER occurred nationwide rather than regionally, and the meteorological factors were included in the simulation, the impact of inter-regional transport of air pollution could be minimized.[48] A more accurate estimate of the impact of inter-regional transport can be quantified by using the source–concentration relationship and inverse model in future studies. Finally, the trained model was used to predict the air pollution during the FLPHER lockdown period. Since only mainstay sectors that maintain the basic human living and society operating were running during the lockdown period, the net differences in air pollution levels between the predicted and real observed results could indicate the reduction degree of air pollution by short-term administrative means of a city under the current energy structure.

In this way, we have obtained the short-term control effect of all the investigated cities. Results show that the average emissions of air pollutants in 174 cities were reduced by 46.9% (15.8 $\mu g/m^3$), 0.59% (0.05 $\mu g/m^3$), 19.2% (11.1 $\mu g/m^3$), and 24.4% (16.6 $\mu g/m^3$) for NO_2, SO_2, $PM_{2.5}$, and PM_{10},

https://doi.org/10.1021/acs.est.0c07170
Environ. Sci. Technol. 2021, 55, 4094−4102

respectively, over the FLPHER lockdown period (see Figure 3). The emission reduction degrees of the air pollutants were also consistent with the degrees of their negative responses to the confirmed COVID-19 cases, as mentioned above (see Figure 2). It has been reported that during the COVID-19 lockdown period the surface transports in freeways and urban roads were decreased by 37%−60%, which can also well-explain the large decline of the NO_2 pollution level observed here.[49] Furthermore, we noticed that the uncertainties of the emission reduction degrees of NO_2 and SO_2 on different dates were relatively small (SD_{NO_2} = ±5.01 $\mu g/m^3$ and SD_{SO_2} = ±1.64 $\mu g/m^3$) during the lockdown period. This might be because the atmospheric NO_2 and SO_2 are predominantly from primary emissions, which are regulated under the uniform national standards. Whereas $PM_{2.5}$ and PM_{10} showed larger variations ($SD_{PM_{2.5}}$ = ± 13.9 $\mu g/m^3$ and $SD_{PM_{10}}$ = ± 18.2 $\mu g/m^3$) probably because their sources are more complex (from both primary emissions and secondary formation from precursor gases, e.g., VOCs).[50,51]

We compared the emission reduction degrees of air pollutants with the results in some existing studies. Compared with the results obtained by a bottom-up method, the reduction of $PM_{2.5}$ in eastern China (19.2%) was very close to that estimated by the Multi-Resolution Emission Inventory Model for China (MEIC) (21%).[52] The NO_2 reduction in the North China Plain obtained here (45.7%) was also close to that estimated by the bottom-up method (51%), and the NO_2 reduction in eastern China (46.9 ± 18.4%) was larger than that in mainland China (31%)[6] but was smaller than that estimated by the bottom-up method (60%−70%).[53] This difference might be attributed to the different corrected emission data used. That is, in this study, the MEIC data set was used in WRF-Chem and the model was trained by altering the emission rates (see the Methods section), while in the bottom-up method, the MEIC emission data was corrected on the basis of dynamic economic and industrial activity levels.[53] In addition, the SO_2 reduction (0.6%) estimated here was smaller than that estimated by the bottom-up method (29%).[52] Furthermore, we also compared the results with the temporally varied statistic data in a previous report that estimated the reduction of air pollution by the FLPHER relative to that before the implementation of FLPHER.[16] The pollution reduction degrees obtained here (46.9% for NO_2, 0.6% for SO_2, 19.2% for $PM_{2.5}$, and 24.4% for PM_{10}) were also consistent with the temporally varied results (46.1% for NO_2, 4.6% for SO_2, 13.7% for $PM_{2.5}$, and 21.8% for PM_{10}).[16]

City-Level Short-Term Emission Control Effect of Air Pollutants in 174 Cities. To make effective regulation policies for individual cities, we separately calculated the short-term control effect (including the direct emission and gaseous precursor emission) of the air pollutants in different cities (Figure 4). Generally, approximately 98.3% of the cities showed a dramatic control effect for NO_2 ranging from −1.54 (−5.05%) to −30.1 $\mu g/m^3$ (−80.8%), and Wenzhou had the maximum reduction effect on NO_2 (Figure 4b). For SO_2, 51.2% of the cities presented an emission reduction ranging from −0.17% to −63.3%, and the maximum reduction on SO_2 was achieved in Ganzhou (Figure 4c). $PM_{2.5}$ showed a control effect in 63.8% of the 174 cities, and the maximum reduction degree reached −60.4% in Wuxi (Figure 4d). PM_{10} showed a control effect in 84.5% of the cities, and the maximum reduction of −61.9% was also found in Wuxi (Figure 4e). Different cities showed distinctly different control effects for different air pollutants, suggesting great regional differences in energy structures and developmental levels.

We compared the emission control effect of air pollutants in the cities stratified by geographic location and city scale. As shown in Figures S4a,b and S5a,b, the cities in Hubei province, which underwent the strictest restriction during the FLPHER period,[9] showed a larger effect for NO_2 and SO_2 reduction probably because the human activities were more constrained in Hubei cities than in other cities. Despite that, out of Hubei, almost an uniform regulation intensity was implemented nationwide during the FLPHER period, and in all these cities, the pollutant emissions have been greatly suppressed. Under such conditions, a slight difference in the FLPHER measures should not have a significant effect on the emission reduction. As shown in Figure S6, no significant correlation was found between the emission control effect and confirmed COVID-19 cases concerning all cities.

Southern cities had a larger control effect for NO_2 and SO_2 than northern cities (Figures S4e,f and S5e,f) due probably to their different energy structures. Furthermore, no significant differences were found in the control effect of NO_2 and SO_2 between megacities and small−medium cities (Figures S4i,j and S5i,j), probably because the general energy structures are similar in megacities and small−medium cities in China (note that countryside regions are not included). For $PM_{2.5}$ and PM_{10}, southern cities and small−medium cities had a larger control effect than northern cities and megacities, but no remarkable difference was found between the cities in and out of Hubei province (Figures S4c,d,g,h,k,l and S5c,d,g,h,k,l).

Species-Specific Short-Term Control Effect. The sources of atmospheric NO_x are normally thought to be related to fossil fuel burning and road traffic.[54] So, the large NO_2 reduction might result from the control of fossil fuel burning or traffic emissions.[55] At the same time, SO_2, which is thought as a proxy of coal burning, showed less reduction effect. This might be attributed to the fact that many sectors associated with SO_2 emission are those that maintain basic life requirements or pillars industries of the national economy. For example, more residential coal heating in northern China due to the COVID-19 lockdowns would marginally offset the reductions by other sources. This was also evidenced by the fact that the COVID-19 lockdowns caused only slight decreases in the fuel processing industries (5.5%), ferrous metal smelting/rolling processing industries (5.6%), and nonferrous metal smelting/rolling processing industries (2.3%).[56]

Regarding particulate matter pollutant, it is necessary to identify the regulation effect on primary particle and gaseous precursor emissions. To probe the responses of $PM_{2.5}$ to the regulation of gaseous precursors (NO_x and VOCs), we performed two WRF-Chem sensitivity tests by altering the emission rates of NO_x and VOCs. As shown in Figure S7, if the anthropogenic NO_x emission is further reduced by 50% than the real situation, the difference between the simulated and observed concentration of $PM_{2.5}$ would decrease from 11.1 (19.2%) to 4.23 $\mu g/m^3$ (8.29%), i.e., the simulated $PM_{2.5}$ level would approximate to the FLPHER-caused "base period" level. If both the anthropogenic emissions of NO_x and VOCs decrease by 50% than the real situation, the $PM_{2.5}$ level would get closer to the "base period" level, with a difference between simulation and observation of only 1.81 $\mu g/m^3$ (3.72%). This result clearly indicates that the reduction of emissions of

https://doi.org/10.1021/acs.est.0c07170
Environ. Sci. Technol. 2021, 55, 4094−4102

precursor gases (e.g., NO_x and VOCs) is an efficient measure to control $PM_{2.5}$ pollution.

Environmental Implications. In recent years, although strong pollution control policies have dramatically decreased the air pollution in China nationwide, the pollution levels still much exceed the WHO guideline limit and the Chinese Ambient Air Quality Standards. More than 180 prefecture-level cities failed to meet the national standard for annual $PM_{2.5}$ level in 2019.[57] Currently, the efforts on further reducing the pollution levels are facing many problems, among which the regional imbalance and unknown effectiveness of regulation policies are the major challenges. The COVID-19-associated FLPHER period provides an unprecedented opportunity to estimate the short-term control effect of different pollutants in different regions. Due to the nearly extreme restrictions on human activities and economical activities, air pollutant emissions were greatly suppressed during the FLPHER period. Thus, such a consequence can represent the reduction degree of air pollution control via short-term administrative means under the current energy structure. This information is important for the prediction of policy effectiveness and policy optimization in different regions.

At present, heavily polluted regions normally receive more strict regulations on all sectors than lightly polluted regions. However, importantly, our results have clearly shown that heavily polluted regions do not necessarily have better effect of air pollutants than lightly polluted regions (see Figure 4). For example, the North China Plain regions suffer from heavier air pollution than the south China but their short-term control effects of air pollutants are much weaker than those of the latter. For a city with a small control effect, excessively stringent measures on the transportation and industry will definitely lead to low efficiency and meaningless economic sacrifices. Thus, the development of emission reduction policies must be specific rather than extensive and ambiguous. Otherwise, even when large economic costs are paid, the policies may not take effect.

For the regions with limited short-term control effect (e.g., the North China Plain), it may be hard to decrease air pollution levels via simply short-term policy regulation. For these regions, long-term strategies and goals should be developed, e.g., optimizing the regional energy structures and improving exhaust gas treatment technologies. Our results also indicate that simply reducing the primary source emission has little effect on $PM_{2.5}$ pollution. More stringent regulation policies should be simultaneously implemented to the aerosol precursor emissions, e.g., VOCs and NO_x. These results provide information to break through the dilemma in the current air pollution control in China and also provide a useful reference for the policymaking in other polluted regions/countries.

■ ASSOCIATED CONTENT

Supporting Information

The Supporting Information is available free of charge at https://pubs.acs.org/doi/10.1021/acs.est.0c07170.

Table of physical and chemical options in the WRF-Chem model used and figures of domain of WRF-Chem modeling, ground mean simulated concentrations, time evolution of the average temperature and average humidity, average changes of air pollution level, short-term emission control effect of air pollutants in the cities, correlation analysis of the confirmed COVID-19 cases with the net changes of the concentrations of the air pollutants, and simulated and observed temporal pollution trends (PDF)

■ AUTHOR INFORMATION

Corresponding Author

Qian Liu − *State Key Laboratory of Environmental Chemistry and Ecotoxicology, Research Center for Eco-Environmental Sciences, Chinese Academy of Sciences, Beijing 100085, China; University of Chinese Academy of Sciences, Beijing 100190, China; Institute of Environment and Health, Jianghan University, Wuhan 430056, China;* orcid.org/0000-0001-8525-7961; Email: qianliu@rcees.ac.cn

Authors

Dawei Lu − *State Key Laboratory of Environmental Chemistry and Ecotoxicology, Research Center for Eco-Environmental Sciences, Chinese Academy of Sciences, Beijing 100085, China; University of Chinese Academy of Sciences, Beijing 100190, China*

Jingwei Zhang − *State Key Laboratory of Atmospheric Boundary Layer Physics and Atmospheric Chemistry, Institute of Atmospheric Physics, Chinese Academy of Sciences, Beijing 100029, China; University of Chinese Academy of Sciences, Beijing 100190, China*

Chaoyang Xue − *State Key Laboratory of Environmental Chemistry and Ecotoxicology, Research Center for Eco-Environmental Sciences, Chinese Academy of Sciences, Beijing 100085, China; University of Chinese Academy of Sciences, Beijing 100190, China*

Peijie Zuo − *State Key Laboratory of Environmental Chemistry and Ecotoxicology, Research Center for Eco-Environmental Sciences, Chinese Academy of Sciences, Beijing 100085, China; University of Chinese Academy of Sciences, Beijing 100190, China*

Zigu Chen − *State Key Laboratory of Environmental Chemistry and Ecotoxicology, Research Center for Eco-Environmental Sciences, Chinese Academy of Sciences, Beijing 100085, China; University of Chinese Academy of Sciences, Beijing 100190, China*

Luyao Zhang − *State Key Laboratory of Environmental Chemistry and Ecotoxicology, Research Center for Eco-Environmental Sciences, Chinese Academy of Sciences, Beijing 100085, China; University of Chinese Academy of Sciences, Beijing 100190, China*

Weibo Ling − *State Key Laboratory of Environmental Chemistry and Ecotoxicology, Research Center for Eco-Environmental Sciences, Chinese Academy of Sciences, Beijing 100085, China; University of Chinese Academy of Sciences, Beijing 100190, China*

Guibin Jiang − *State Key Laboratory of Environmental Chemistry and Ecotoxicology, Research Center for Eco-Environmental Sciences, Chinese Academy of Sciences, Beijing 100085, China; University of Chinese Academy of Sciences, Beijing 100190, China;* orcid.org/0000-0002-6335-3917

Complete contact information is available at: https://pubs.acs.org/10.1021/acs.est.0c07170

Author Contributions

D.L., Q.L., and G.J. conceived and designed the research. D.L., J.Z., and C.X. performed data analyses and produced the

https://doi.org/10.1021/acs.est.0c07170
Environ. Sci. Technol. 2021, 55, 4094−4102

figures. J.Z. and D.L. performed and analyzed WRF-Chem simulations. D.L., P.Z., Z.C., L.Z., and W.L. collected the data used in this study. D.L. and Q.L. conducted the scientific discussions and wrote the paper.

Notes

The authors declare no competing financial interest.

■ ACKNOWLEDGMENTS

This work was financially supported by the National Natural Science Foundation of China (Nos. 21904134, 91843301, 21825403, 21976194, 92043302), the Chinese Academy of Sciences (Nos. ZDBS-LY-DQC030 and QYZDB-SSW-DQC018), the Strategic Priority Research Program of CAS, and the Ozone Formation Mechanism and Control Strategies Project of Research Center for Eco-Environmental Sciences, CAS (No. RCEES-CYZX-2020), and the Sanming Project of Medicine in Shenzhen (No. SZSM201811070).

■ REFERENCES

(1) Cohen, A. J.; Brauer, M.; Burnett, R.; et al. Estimates and 25-year trends of the global burden of disease attributable to ambient air pollution: an analysis of data from the Global Burden of Diseases Study 2015. *Lancet.* **2017**, *389* (10082), 1907−1918.

(2) Huang, R. J.; Zhang, Y.; Bozzetti, C.; Ho, K. F.; Cao, J. J.; Han, Y.; Daellenbach, K. R.; Slowik, J. G.; Platt, S. M.; Canonaco, F.; Zotter, P.; Wolf, R.; Pieber, S. M.; Bruns, E. A.; Crippa, M.; Ciarelli, G.; Piazzalunga, A.; Schwikowski, M.; Abbaszade, G.; Schnelle-Kreis, J.; Zimmermann, R.; An, Z.; Szidat, S.; Baltensperger, U.; Haddad, I. E.; Prevot, A. S. High secondary aerosol contribution to particulate pollution during haze events in China. *Nature* **2014**, *514* (7521), 218−222.

(3) State Council of the People's Republic of China. Notice of the general office of the state council on issuing the air pollution prevention and control action plan. http://www.gov.cn/zwgk/2013-09/12/content_2486773.htm (accessed 2019-08-21).

(4) Ministry of Ecology and Environment of the People's Republic of China. 2017 Report on the state of the ecology and environment in China. http://english.mee.gov.cn/Resources/Reports/soe/SOEE2017/201808/P020180801597738742758.pdf (accessed 2019-10-28).

(5) Zhang, Q.; Zheng, Y.; Tong, D.; Shao, M.; Wang, S.; Zhang, Y.; Xu, X.; Wang, J.; He, H.; Liu, W.; Ding, Y.; Lei, Y.; Li, J.; Wang, Z.; Zhang, X.; Wang, Y.; Cheng, J.; Liu, Y.; Shi, Q.; Yan, L.; Geng, G.; Hong, C.; Li, M.; Liu, F.; Zheng, B.; Cao, J.; Ding, A.; Gao, J.; Fu, Q.; Huo, J.; Liu, B.; Liu, Z.; Yang, F.; He, K.; Hao, J. Drivers of improved PM2.5 air quality in China from 2013 to 2017. *Proc. Natl. Acad. Sci. U. S. A.* **2019**, *116* (49), 24463−24469.

(6) Xing, J.; Li, S.; Jiang, Y.; Wang, S.; Ding, D.; Dong, Z.; Zhu, Y.; Hao, J. Quantifying the emission changes and associated air quality impacts during the COVID-19 pandemic in North China Plain: a response modeling study. *Atmos. Chem. Phys.* **2020**, *20* (22), 14347−14359.

(7) Yang, X.; Lu, D.; Tan, J.; Sun, X.; Zhang, Q.; Zhang, L.; Li, Y.; Wang, W.; Liu, Q.; Jiang, G. Two-Dimensional Silicon Fingerprints Reveal Dramatic Variations in the Sources of Particulate Matter in Beijing during 2013−2017. *Environ. Sci. Technol.* **2020**, *54* (12), 7126−7135.

(8) Wang, C.; Horby, P. W.; Hayden, F. G.; Gao, G. F. A novel coronavirus outbreak of global health concern. *Lancet* **2020**, *395* (10223), 470−473.

(9) Xinhua News. 30 provinces activated First-level Public Health Emergency Response. http://www.xinhuanet.com/politics/2020-01/25/c_1125502232.htm (accessed 2020-01-25).

(10) Xinhua News. Traffic system works well in the seventh day of the Spring Festival holiday. http://www.xinhuanet.com/politics/2020-01/30/c_1125514185.htm (accessed 2020-01-30).

(11) Cohen, J.; Kupferschmidt, K. Strategies shift as coronavirus pandemic looms. *Science* **2020**, *367* (6481), 962−963.

(12) Lelieveld, J.; Evans, J. S.; Fnais, M.; Giannadaki, D.; Pozzer, A. The contribution of outdoor air pollution sources to premature mortality on a global scale. *Nature* **2015**, *525* (7569), 367−371.

(13) Pei, Z.; Han, G.; Ma, X.; Su, H.; Gong, W. Response of major air pollutants to COVID-19 lockdowns in China. *Sci. Total Environ.* **2020**, *743*, 140879.

(14) Yang, Y.; Ren, L.; Li, H.; Wang, H.; Wang, P.; Chen, L.; Yue, X.; Liao, H. Fast Climate Responses to Aerosol Emission Reductions During the COVID-19 Pandemic. *Geophys. Res. Lett.* **2020**, *47* (19), No. e2020GL089788.

(15) Dai, Q.; Liu, B.; Bi, X.; Wu, J.; Liang, D.; Zhang, Y.; Feng, Y.; Hopke, P. K. Dispersion Normalized PMF Provides Insights into the Significant Changes in Source Contributions to $PM_{2.5}$ after the COVID-19 Outbreak. *Environ. Sci. Technol.* **2020**, *54* (16), 9917−9927.

(16) Zhao, Y.; Zhang, K.; Xu, X.; Shen, H.; Zhu, X.; Zhang, Y.; Hu, Y.; Shen, G. Substantial Changes in Nitrogen Dioxide and Ozone after Excluding Meteorological Impacts during the COVID-19 Outbreak in Mainland China. *Environ. Sci. Technol. Lett.* **2020**, *7* (6), 402−408.

(17) He, G.; Pan, Y.; Tanaka, T. The short-term impacts of COVID-19 lockdown on urban air pollution in China. *Nat. Sustain.* **2020**, *3*, 1005−1011.

(18) Sun, Y.; Lei, L.; Zhou, W.; Chen, C.; He, Y.; Sun, J.; Li, Z.; Xu, W.; Wang, Q.; Ji, D.; Fu, P.; Wang, Z.; Worsnop, D. R. A chemical cocktail during the COVID-19 outbreak in Beijing, China: Insights from six-year aerosol particle composition measurements during the Chinese New Year holiday. *Sci. Total Environ.* **2020**, *742*, 140739.

(19) Lian, X.; Huang, J.; Huang, R.; Liu, C.; Wang, L.; Zhang, T. Impact of city lockdown on the air quality of COVID-19-hit of Wuhan city. *Sci. Total Environ.* **2020**, *742*, 140556.

(20) Liu, Z.; Ciais, P.; Deng, Z.; Lei, R.; Davis, S. J.; Feng, S.; Zheng, B.; Cui, D.; Dou, X.; Zhu, B.; Guo, R.; Ke, P.; Sun, T.; Lu, C.; He, P.; Wang, Y.; Yue, X.; Wang, Y.; Lei, Y.; Zhou, H.; Cai, Z.; Wu, Y.; Guo, R.; Han, T.; Xue, J.; Boucher, O.; Boucher, E.; Chevallier, F.; Tanaka, K.; Wei, Y.; Zhong, H.; Kang, C.; Zhang, N.; Chen, B.; Xi, F.; Liu, M.; Bréon, F.-M.; Lu, Y.; Zhang, Q.; Guan, D.; Gong, P.; Kammen, D. M.; He, K.; Schellnhuber, H. J. Near-real-time monitoring of global CO2 emissions reveals the effects of the COVID-19 pandemic. *Nat. Commun.* **2020**, *11* (1), 5172.

(21) Liu, F.; Page, A.; Strode, S. A.; Yoshida, Y.; Choi, S.; Zheng, B.; Lamsal, L. N.; Li, C.; Krotkov, N. A.; Eskes, H.; van der A, R.; Veefkind, P.; Levelt, P. F.; Hauser, O. P.; Joiner, J. Abrupt decline in tropospheric nitrogen dioxide over China after the outbreak of COVID-19. *Sci. Adv.* **2020**, *6* (28), No. eabc2992.

(22) Zhang, Q.; Pan, Y.; He, Y.; Walters, W. W.; Ni, Q.; Liu, X.; Xu, G.; Shao, J.; Jiang, C. Substantial nitrogen oxides emission reduction from China due to COVID-19 and its impact on surface ozone and aerosol pollution. *Sci. Total Environ.* **2021**, *753*, 142238.

(23) Feng, S.; Jiang, F.; Wang, H.; Wang, H.; Ju, W.; Shen, Y.; Zheng, Y.; Wu, Z.; Ding, A. NOx Emission Changes Over China During the COVID-19 Epidemic Inferred From Surface NO2 Observations. *Geophys. Res. Lett.* **2020**, *47* (19), No. e2020GL090080.

(24) Wang, Y.; Wen, Y.; Wang, Y.; Zhang, S.; Zhang, K. M.; Zheng, H.; Xing, J.; Wu, Y.; Hao, J. Four-Month Changes in Air Quality during and after the COVID-19 Lockdown in Six Megacities in China. *Environ. Sci. Technol. Lett.* **2020**, *7* (11), 802−808.

(25) Yin, Z.; Zhang, Y.; Wang, H.; Li, Y. Evident PM2.5 Drops in the East of China due to the COVID-19 Quarantines in February. *Atmos. Chem. Phys. Discuss.* **2020**, *21* (3), 1581−1592.

(26) Kim, H. C.; Kim, S.; Cohen, M.; Bae, C.; Lee, D.; Saylor, R.; Bae, M.; Kim, E.; Kim, B. U.; Yoon, J. H.; Stein, A. Quantitative assessment of changes in surface particulate matter concentrations over China during the COVID-19 pandemic and their implications for Chinese economic activity. *Atmos. Chem. Phys. Discuss.*, in press, **2020**.

(27) Chauhan, A.; Singh, R. P. Decline in PM2.5 concentrations over major cities around the world associated with COVID-19. *Environ. Res.* **2020**, *187*, 109634.

https://doi.org/10.1021/acs.est.0c07170
Environ. Sci. Technol. 2021, 55, 4094−4102

(28) Singh, R. P.; Chauhan, A. Impact of lockdown on air quality in India during COVID-19 pandemic. *Air Qual., Atmos. Health* **2020**, *13* (8), 921−928.
(29) Le, T.; Wang, Y.; Liu, L.; Yang, J.; Yung, Y. L.; Li, G.; Seinfeld, J. H. Unexpected air pollution with marked emission reductions during the COVID-19 outbreak in China. *Science* **2020**, *369* (6504), 702−706.
(30) Wang, S. X.; Zhao, M.; Xing, J.; Wu, Y.; Zhou, Y.; Lei, Y.; He, K. B.; Fu, L. X.; Hao, J. M. Quantifying the Air Pollutants Emission Reduction during the 2008 Olympic Games in Beijing. *Environ. Sci. Technol.* **2010**, *44* (7), 2490−2496.
(31) Huang, K.; Zhang, X. Y.; Lin, Y. F. The "APEC Blue" phenomenon: Regional emission control effects observed from space. *Atmos. Res.* **2015**, *164*, 65−75.
(32) Grell, G. A.; Peckham, S. E.; Schmitz, R.; McKeen, S. A.; Frost, G.; Skamarock, W. C.; Eder, B. Fully coupled "online" chemistry within the WRF model. *Atmos. Environ.* **2005**, *39* (37), 6957−6975.
(33) Li, G.; Lei, W.; Zavala, M.; Volkamer, R.; Dusanter, S.; Stevens, P.; Molina, L. T. Impacts of HONO sources on the photochemistry in Mexico City during the MCMA-2006/MILAGO Campaign. *Atmos. Chem. Phys.* **2010**, *10* (14), 6551−6567.
(34) Zhang, J. W.; An, J. L.; Qu, Y.; Liu, X. G.; Chen, Y. Impacts of potential HONO sources on the concentrations of oxidants and secondary organic aerosols in the Beijing-Tianjin-Hebei region of China. *Sci. Total Environ.* **2019**, *647*, 836−852.
(35) National Centers for Environmental Prediction/National Weather Service/NOAA/U.S. Department of Commerce. NCEP FNL Operational Model Global Tropospheric Analyses, continuing from July 1999. *Research Data Archive at the National Center for Atmospheric Research, Computational and Information Systems Laboratory*, **2000**, updated daily.
(36) Whole Atmosphere Community Climate Model (WACCM). https://www.acom.ucar.edu/waccm/download.shtml (accessed 2020-05-21).
(37) Zhang, Q.; Streets, D. G.; Carmichael, G. R.; He, K. B.; Huo, H.; Kannari, A.; Klimont, Z.; Park, I. S.; Reddy, S.; Fu, J. S.; Chen, D.; Duan, L.; Lei, Y.; Wang, L. T.; Yao, Z. L. Asian emissions in 2006 for the NASA INTEX-B mission. *Atmos. Chem. Phys.* **2009**, *9* (14), 5131−5153.
(38) Li, M.; Zhang, Q.; Kurokawa, J.; Woo, J. H.; He, K. B.; Lu, Z. F.; Ohara, T.; Song, Y.; Streets, D. G.; Carmichael, G. R.; Cheng, Y. F.; Hong, C. P.; Huo, H.; Jiang, X. J.; Kang, S. C.; Liu, F.; Su, H.; Zheng, B. MIX: a mosaic Asian anthropogenic emission inventory under the international collaboration framework of the MICS-Asia and HTAP. *Atmos. Chem. Phys.* **2017**, *17* (2), 935−963.
(39) Dong, W.-X.; Xing, J.; Wang, S.-X. Temporal and spatial distribution of anthropogenic ammonia emissions in China: 1994−2006. *Environ. Sci.* **2010**, *31* (7), 1457−1463.
(40) Huang, X.; Li, M. M.; Li, J. F.; Song, Y. A high-resolution emission inventory of crop burning in fields in China based on MODIS Thermal Anomalies/Fire products. *Atmos. Environ.* **2012**, *50*, 9−15.
(41) Guenther, A. B.; Jiang, X.; Heald, C. L.; Sakulyanontvittaya, T.; Duhl, T.; Emmons, L. K.; Wang, X. The Model of Emissions of Gases and Aerosols from Nature version 2.1 (MEGAN2.1): an extended and updated framework for modeling biogenic emissions. *Geosci. Model Dev.* **2012**, *5* (6), 1471−1492.
(42) Levy, M.; Zhang, R. Y.; Zheng, J.; Zhang, A. L.; Xu, W.; Gomez-Hernandez, M.; Wang, Y.; Olaguer, E. Measurements of nitrous acid (HONO) using ion drift-chemical ionization mass spectrometry during the 2009 SHARP field campaign. *Atmos. Environ.* **2014**, *94*, 231−240.
(43) Seinfeld, J. H.; Pandis, P. N. *Atmospheric Chemistry and Physics: From Air Pollution to Climate Change*; John Wiley & Sons, 2016.
(44) Central people's government of the people's republic of China. Notice of the State Council on readjustment of the Standards for The Division of Urban Dimensions. http://www.gov.cn/zhengce/content/2014-11/20/content_9225.htm (accessed 2020-06-22).
(45) Foley, K. M.; Roselle, S. J.; Appel, K. W.; Bhave, P. V.; Pleim, J. E.; Otte, T. L.; Mathur, R.; Sarwar, G.; Young, J. O.; Gilliam, R. C.; Nolte, C. G.; Kelly, J. T.; Gilliland, A. B.; Bash, J. O. Incremental testing of the Community Multiscale Air Quality (CMAQ) modeling system version 4.7. *Geosci. Model Dev.* **2010**, *3* (1), 205−226.
(46) Li, G.; Lei, W.; Bei, N.; Molina, L. T. Contribution of garbage burning to chloride and $PM_{2.5}$ in Mexico City. *Atmos. Chem. Phys.* **2012**, *12* (18), 8751−8761.
(47) Li, G.; Zavala, M.; Lei, W.; Tsimpidi, A. P.; Karydis, V. A.; Pandis, S. N.; Canagaratna, M. R.; Molina, L. T. Simulations of organic aerosol concentrations in Mexico City using the WRF-CHEM model during the MCMA-2006/MILAGRO campaign. *Atmos. Chem. Phys.* **2011**, *11* (8), 3789−3809.
(48) Huang, X.; Ding, A.; Wang, Z.; Ding, K.; Gao, J.; Chai, F.; Fu, C. Amplified transboundary transport of haze by aerosol-boundary layer interaction in China. *Nat. Geosci.* **2020**, *13* (6), 428−434.
(49) Lv, Z.; Wang, X.; Deng, F.; Ying, Q.; Archibald, A. T.; Jones, R. L.; Ding, Y.; Cheng, Y.; Fu, M.; Liu, Y.; Man, H.; Xue, Z.; He, K.; Hao, J.; Liu, H. Source-Receptor Relationship Revealed by the Halted Traffic and Aggravated Haze in Beijing during the COVID-19 Lockdown. *Environ. Sci. Technol.* **2020**, *54* (24), 15660−15670.
(50) Wu, D.; Ding, X.; Li, Q.; Sun, J. F.; Huang, C.; Yao, L.; Wang, X. M.; Ye, X. N.; Chen, Y. J.; He, H.; Chen, J. M. Pollutants emitted from typical Chinese vessels: Potential contributions to ozone and secondary organic aerosols. *J. Clean Prod.* **2019**, *238*, 117862.
(51) Zhu, Y. H.; Yang, L. X.; Chen, J. M.; Wang, X. F.; Xue, L. K.; Sui, X.; Wen, L.; Xu, C. H.; Yao, L.; Zhang, J. M.; Shao, M.; Lu, S. H.; Wang, W. X. Characteristics of ambient volatile organic compounds and the influence of biomass burning at a rural site in Northern China during summer 2013. *Atmos. Environ.* **2016**, *124*, 156−165.
(52) Zheng, B.; Zhang, Q.; Geng, G.; Shi, Q.; Lei, Y.; He, K. Changes in China's anthropogenic emissions during the COVID-19 pandemic. *Earth Syst. Sci. Data Discuss.*, in press, **2020**.
(53) Huang, X.; Ding, A.; Gao, J.; Zheng, B.; Zhou, D.; Qi, X.; Tang, R.; Wang, J.; Ren, C.; Nie, W.; Chi, X.; Xu, Z.; Chen, L.; Li, Y.; Che, F.; Pang, N.; Wang, H.; Tong, D.; Qin, W.; Cheng, W.; Liu, W.; Fu, Q.; Liu, B.; Chai, F.; Davis, S. J.; Zhang, Q.; He, K. Enhanced secondary pollution offset reduction of primary emissions during COVID-19 lockdown in China. *Natl. Sci. Rev.* **2020**, *8* (2), nwaa137.
(54) Dong, Y.; Xu, L.; Yang, Z.; Zheng, H.; Chen, L. Aggravation of reactive nitrogen flow driven by human production and consumption in Guangzhou City China. *Nat. Commun.* **2020**, *11* (1), 1209.
(55) Tanzer-Gruener, R.; Li, J.; Eilenberg, S. R.; Robinson, A. L.; Presto, A. A. Impacts of Modifiable Factors on Ambient Air Pollution: A Case Study of COVID-19 Shutdowns. *Environ. Sci. Technol. Lett.* **2020**, *7* (8), 554−559.
(56) Industrial economic data in China. https://www.wind.com.cn/NewSite/edb.html (accessed 2020-04-25).
(57) Ministry of Ecology and Environment of the People's Republic of China. An overview of ecological and environmental quality in 2019. http://www.gov.cn/xinwen/2020-05/08/content_5509650.htm (accessed 2020-05-08).

https://doi.org/10.1021/acs.est.0c07170
Environ. Sci. Technol. 2021, 55, 4094−4102